AIMS Mathematics, 11(11): 39459–39476.
DOI: 10.3934/math.20261519
Received: 10 September 2026
Revised: 08 November 2026
Accepted: 16 November 2026
Published: 25 November 2026

http://www.aimspress.com/journal/Math

Research article

Soliton dynamics and continuous dependence on the kernel in the (3+1)-dimensional Jimbo-Miwa equation via local generalized derivative operators

Juan E. Nápoles V[1], Hadeel Bin Amer[2], Aziz Khan[3,*], Aiman Mukheimer[3] and Shahneela Pitafi[4]

[1] UNNE, FaCENA, Ave. Libertad 5450, Corrientes 3400, Argentina; and UTN-FRRE, French 414, Resistencia, Chaco 3500, Argentina

[2] Department of Computer Science, College of Computer and Information Sciences, Majmaah University, Al-Majmaah 11952, Saudi Arabia

[3] Department of Mathematics and Sciences, Prince Sultan University, P.O. Box 66833, Riyadh 11586, Saudi Arabia

[4] Faculty of Data Science and Information Technology, INTI International University, Negeri Sembilan, Malaysia

* **Correspondence:** Email: azizkhan927@yahoo.com, akhan@psu.edu.sa; Tel: +966531233923.

Abstract: This work investigates the propagation of nonlinear waves in the (3+1)-dimensional Jimbo–Miwa (JM) equation in which the time derivative is replaced by the local generalized derivative (LGD), $D_N^{\sigma} = N(t,\sigma)\partial_t$. Initially, we emphasize that the explicit LGD is a local operator: on any interval where $N > 0$, it is equivalent to an ordinary derivative with respect to the reparametrized time $\tau(t) = \int_0^t ds/N(s,\sigma)$, so it represents no hereditary (memory) effects. Within this theoretical formulation, we derive a traveling-wave reduction that maintains the integration constant, substantiate the algebraic compatibility condition that the coefficients are required to fulfill, and obtain, with explicit parameter restrictions, bright (and dark) pulses with their bounded kink potentials, cnoidal periodic waves, and singular periodic, hyperbolic, and rational solutions. The kernel does not alter the spatial profiles; it governs the kinematics of the front. We show that exponential kernels arrest the front at a finite position, conformable kernels give sublinear propagation, and Mittag-Leffler kernel functions generate a propagating front that starts from rest and approaches the classical speed with a power-law lag. We show that the energy and Shannon entropy of the profiles are invariant for every kernel. Finally, we prove existence and uniqueness for Cauchy problems driven by the LGD via a contraction argument in a weighted Banach space, and derive explicit Lipschitz estimates for the dependence of solutions on the kernel parameter as process innovation.

Keywords: local generalized derivative (LGD); Jimbo-Miwa equation; soliton solutions; time

reparametrization; continuous dependence; nonlinear evolution equations
Mathematics Subject Classification: 35Q53, 26A33, 35C07, 37K40

1. Introduction

The modeling of nonlinear phenomena in continuous media has undergone a revolution thanks to the development of nonclassical differential operators. While traditional fractional calculus (Riemann-Liouville, Caputo) has allowed for the capture of global memory effects [1, 2], its application often leads to complications in the product and chain rules. In this context, the local generalized derivative (LGD) emerges as a simple alternative that, by means of a continuous weight (kernel), governs a smooth transition between the classical derivative and various conformable-type derivatives without losing the operational structure linearity, Leibniz, and chain rules of the local calculus.

The generalized derivative was defined in [3], in the following way (see also [4, 5]).

Definition 1. Given a function $F : [0, +\infty) \to \mathbb{R}$, then the N-derivative of F of order β is defined by

$$D_N^\beta F(t) = \lim_{h\to 0} \frac{F(t + hN(t,\beta)) - F(t)}{h}$$

for all $t > 0, \beta \in (0, 1)$, and $N(t,\beta)$ is some absolutely continuous and positive function.

If F is N-differentiable in some $(0, \sigma)$, and $\lim_{t\to 0^+} D_N^\beta F(t)$ exists, then define $D_N^\beta F(0) = \lim_{t\to 0^+} D_N^\beta F(t)$. Note that if F is differentiable, then

$$D_N^\beta F(t) = N(t,\beta)F'(t),$$

where $F'(t)$ is the ordinary derivative.

Since $D_N^\beta F(t) = N(t,\beta)F'(t)$ depends only on the value of F' at the present instant t, the LGD is a *local* operator. This is the essential difference with the Riemann-Liouville or Caputo derivatives, which are convolution operators with a singular (power-law) kernel and therefore depend on the whole history of F on $[0, t]$ [1]. In particular, the LGD cannot by itself describe hereditary (memory) effects. A useful way to read it is as a change of clock: Wherever $N(\cdot,\beta) > 0$, setting $\tau(t) = \int_{t_0}^t ds/N(s,\beta)$ gives $D_N^\beta = d/d\tau$. Accordingly, throughout this revised version, the word "kernel" refers only to the weight N, and the effects of N are interpreted as a nonuniform time scale, not as memory.

This definition recovers the conventional operator when $N(t,\beta) = 1$, and also allows other weights, such as power, exponential, or Mittag-Leffler weights. As shown in Sections 3 and 4, these weights do not modify the spatial shape of traveling waves, but they change the kinematics of the wave fronts (acceleration, deceleration, or arrest).

The space, which we will denote as $\mathcal{D}_N^\beta(I)$, must guarantee that the operator is well-defined and manageable.

Definition 2. Let $I = [0, T]$ be a compact interval and let $N : I \times (0, 1] \to \mathbb{R}^+$ be a weight such that $N(\cdot,\beta)$ is continuous on I and satisfies $0 < n_* \le N(t,\beta) \le n^* < \infty$ for $t \in I$. We say that $F : I \to \mathbb{R}$

belongs to $\mathcal{D}_N^\beta(I)$ if $F \in C^1(I)$, one-sided derivatives at the end points. For such F, the limit defining $D_N^\beta F(t)$ exists for every $t \in I$,

$$D_N^\beta F(t) = N(t,\beta)F'(t),$$

and $D_N^\beta F$ is continuous on I, because it is the product of the two continuous functions $N(\cdot,\beta)$ and F'. Ordinary differentiability alone would not suffice for this continuity; continuity of F' is needed.

If $N(t,\beta)$ tends to zero or to infinity at some point of I, the two-sided bounds, fail and one must work with weighted spaces and more careful boundary conditions. The existence results of Section 5 are formulated directly in terms of $\rho = 1/N$, which only needs to be bounded and continuous.

We will define the norm in this space as:

$$\|F\|_{\mathcal{D}_N^\beta} = \sup_{t\in I}|F(t)| + \sup_{t\in I}|D_N^\beta F(t)|.$$

Since $\min\{1, n_*\}\|F\|_{C^1(I)} \le \|F\|_{\mathcal{D}_N^\beta} \le \max\{1, n^*\}\|F\|_{C^1(I)}$, with $\|F\|_{C^1(I)} = \sup|F| + \sup|F'|$, this norm is equivalent to the usual C^1 norm, and $\mathcal{D}_N^\beta(I)$ is a Banach space (Lemma 18 in Section 5).

The generalized derivative presented above has proven useful in several applied problems (see [6–10]).

It is clear that if we choose $N(t,\beta) = t^{1-\beta}$, we recover the derivative of [10], with $N(t,\beta) = e^{t^{-\beta}}$ we obtain the non-conformable derivative of [11, 12]. If put $N(t,\beta) = (t + \frac{1}{\Gamma(\beta)})^{1-\beta}$ then we have the β-derivative defined, and if $N(t,\beta) = 1$, we have the classic derivative. However, the framework of [3] allows for more general weights, which correspond to variable time scales that the simple conformable derivative does not cover [13–15].

In this paper, we shall use the Mittag-Leffler function

$$E_\sigma(z) = \sum_{k=0}^{\infty} \frac{z^k}{\Gamma(\sigma k + 1)}, \qquad 0 < \sigma \le 1, \tag{1.1}$$

and, throughout the whole manuscript, the Mittag-Leffler weight is always $N(t,\sigma) = E_\sigma(t^{-\sigma})$, $t > 0$. For $z \ge 0$, $E_\sigma(z) \ge 1$ is increasing, $E_\sigma(z) = 1 + z/\Gamma(1+\sigma) + O(z^2)$ as $z \to 0^+$, and $E_\sigma(z) \sim \sigma^{-1}\exp(z^{1/\sigma})$ as $z \to +\infty$ [2]. Consequently $\rho(t) = 1/E_\sigma(t^{-\sigma})$ is continuous and increasing on $(0,\infty)$, $0 < \rho < 1$, $\rho(t) \sim \sigma e^{-1/t}$ as $t \to 0^+$ (so that ρ extends continuously by $\rho(0) = 0$), and $\rho(t) \to 1$ as $t \to \infty$. In particular $\int_0^t \rho(s)\,ds$ is finite, which justifies the lower limit $t = 0$ used below.

From [16], we can define the generalized partial derivatives as follows.

Definition 3. Given a real-valued function $f : \mathbb{R}^n \to \mathbb{R}$ and $\overrightarrow{a} = (a_1, \ldots, a_n) \in \mathbb{R}^n$ a point whose *ith* component is positive, then the generalized partial N-derivative of f of order β with respect to the variable x_i, at the point $\overrightarrow{a} = (a_1, \ldots, a_n)$, denoted ${}_iD_N^\beta f(\overrightarrow{a})$, and called the *ith* generalized partial derivative of f of the order $\beta \in (0,1]$ at $\overrightarrow{a}$, is defined by

$${}_iD_N^\beta f(\overrightarrow{a}) = \lim_{\varepsilon\to 0}\frac{f(a_1, \ldots, a_i + \varepsilon N_i(a_i,\beta), \ldots, a_n) - f(a_1, \ldots, a_i, \ldots, a_n)}{\varepsilon}$$

if the limit exists.

Remark 4. When using functions of two independent variables, we will only indicate the variable with respect to which we are differentiating, so ${}_tD_N^\beta$ will indicate the first-order partial derivative with respect to the variable t.

Remark 5. If a real-valued function f with n variables has all generalized partial derivatives of the order $\beta \in (0, 1]$ at $\overrightarrow{a}$, each $a_i > 0$, then the generalized β-gradient of f of the order $\beta \in (0, 1]$ at $\overrightarrow{a}$ is

$$\nabla_N^\beta f(\overrightarrow{a}) = ({}_1D_N^\beta f(\overrightarrow{a}), \ldots, {}_n D_N^\beta f(\overrightarrow{a})).$$

Remark 6. The higher-order N-partial derivatives of a real-valued function f with n variables, with $\beta \in (0, 1]$ at $\overrightarrow{a}$, are similarly defined by

$${}_iD_N^\beta \left({}_iD_N^\beta f\right) =_{(i,i)} D_N^{\beta+\beta} f.$$

Let $F = (F_1, F_2, \ldots, F_n)$ be a differentiable vector field on an open set $\Omega \subset \mathbb{R}^n$. The generalized local divergence is defined as the sum of the generalized partial derivatives:

$$\mathrm{div}_N^\beta F = \sum_{i=1}^{n} D_{N,x_i}^\beta F_i = \sum_{i=1}^{n} N(x_i, \beta) \frac{\partial F_i}{\partial x_i}.$$

We define the generalized integral associated with the LGD as:

$$\mathcal{I}_N^\beta f(t) = \int_a^t \frac{f(x)}{N(x, \beta)} dx,$$

where $N(x, \beta)$ is the kernel defined in the work [3]. If $N(x, \beta) = x^{1-\beta}$, we recover the conformable operator, and if $N(x, \beta) = 1$, we obtain the classic Riemann integral, to cite just two specific examples of this operator.

In [6], the following time-fractional (3+1)-dimensional Jimbo-Miwa (JM) equation was studied:

$$\varphi_{xxxy} + \kappa \varphi_{xy} \varphi_x + \omega \varphi_{xx} \varphi_y + r D_t^\sigma (\varphi_y) - \mu \varphi_{xz} = 0,$$

where $\varphi(x; y; z; t)$ is a real-valued wave function, describing the height of waves, κ, ω, r, and μ are real constants, and $\mathcal{D}_t^\sigma$ is the conformable derivative of [10] defined in this way:

$$\mathcal{D}_t^\sigma u(t, x) = \lim_{\epsilon \to 0} \frac{u(t + \epsilon t^{1-\sigma}, x) - u(t, x)}{\epsilon} = t^{1-\sigma} \frac{\partial u}{\partial t}.$$

In this work, we will study the generalized (3+1)-dimensional JM equation:

$$\varphi_{xxxy} + \kappa \varphi_{xy} \varphi_x + \omega \varphi_{xx} \varphi_y + r D_{N,t}^\sigma (\varphi_y) - \mu \varphi_{xz} = 0, \quad 0 < \sigma \leq 1, \tag{1.2}$$

where κ, ω, r and μ are real constants, and

$$D_{N,t}^\sigma u(t, x) = N(t, \sigma) \frac{\partial u}{\partial t}$$

is the generalized time derivative.

The JM equation [17], as one of the fundamental members of the Kadomtsev-Petviashvili hierarchy, describes pressure waves in fluids and dynamics in plasma lattices. Replacing ∂_t by the LGD amounts to letting the medium advance on a nonuniform time scale, a simple way of describing media in which the effective propagation speed varies in time (for instance, because of aging or slow external driving), without introducing nonlocal operators.

Exact solutions and symmetry reductions of time-fractional nonlinear evolution equations have attracted considerable attention. Lie symmetry analysis, optimal systems, and invariant solutions have recently been obtained for several time-fractional models [18–20], and soliton solutions of the conformable (3+1)-dimensional JM equation were obtained in [6]. Since the derivatives used in [18–20] are nonlocal, those reductions differ structurally from the one obtained here, where the operator is local.

The central problem of this research is to determine how replacing the classical time derivative with the LGD alters the existence, shape, and propagation of soliton solutions, and what can be proved rigorously about the dependence of solutions on the kernel. Our contributions are as follows. (i) We make explicit that (1.2) is equivalent, via $\tau(t)$, to the classical JM equation (Proposition 7); hence the spatial profiles coincide with the classical ones, and all of the novelty lies in the time kinematics. (ii) We give a complete and corrected traveling-wave analysis that keeps the integration constant and states the compatibility condition and the parameter restrictions for every family. (iii) We classify the front kinematics according to the asymptotics of $\tau(t)$ (uniform, sublinear, arrested, or delayed). (iv) We prove that energy and entropy are invariant, which corrects the dissipation interpretation. (v) We prove existence and uniqueness for Cauchy problems driven by the LGD, together with explicit Lipschitz estimates with respect to the kernel parameter. Compared with [6], the conformable case $N = t^{1-\sigma}$ is recovered as a particular weight, but the results (ii)–(v) are not contained there.

2. Results

Proposition 7. *Let $N(\cdot,\sigma)$ be continuous and positive on $(0,T]$ with $\rho = 1/N$ integrable on $(0,T]$, and let $\tau(t) = \int_0^t \rho(s,\sigma)\,ds$. Then $\tau : [0,T] \to [0,\tau(T)]$ is a strictly increasing bijection, and a sufficiently smooth function $\varphi(x,y,z,t)$ solves (1.2) on $\mathbb{R}^3 \times (0,T]$ if and only if $\psi(x,y,z,\tau) := \varphi(x,y,z,t(\tau))$ solves the classical JM equation*

$$\psi_{xxxy} + \kappa\psi_{xy}\psi_x + \omega\psi_{xx}\psi_y + r\,\psi_{y\tau} - \mu\psi_{xz} = 0 \tag{2.1}$$

on $\mathbb{R}^3 \times (0,\tau(T)]$.

Proof. Since $\tau'(t) = \rho(t,\sigma) > 0$ on $(0,T]$, τ is strictly increasing and has a continuous inverse. By the chain rule, $\partial_t\varphi = \rho\,\partial_\tau\psi$, hence $D^{\sigma}_{N,t}\varphi_y = N\rho\,\psi_{y\tau} = \psi_{y\tau}$. The spatial derivatives are not affected, so (1.2) and (2.1) coincide. □

Remark 8. Proposition 7 has three consequences that we use throughout. (a) The LGD introduces no dependence on past states, so any physical interpretation must be phrased in terms of a time-dependent clock and not in terms of memory, hysteresis, or viscoelastic dissipation. (b) Every solution of the classical equation (2.1) gives a solution of (1.2), and every quantity conserved by (2.1) is also conserved by (1.2) (Section 4). (c) Existence and uniqueness results for (2.1) on $[0,\tau(T)]$ transfer directly to (1.2) on $[0,T]$. The results of [6] correspond to $\tau(t) = t^{\sigma}/\sigma$.

Traveling-wave reduction

Theorem 9. *(Theorem of reduction to ordinary differential equation (ODE)) Let $\sigma_1, \beta \neq 0$ and $\kappa + \omega \neq 0$. The traveling wave transformation*

$$\varphi(x,y,z,t) = U(\varsigma),$$

$$\varsigma = \sigma_1 x + \beta y + \lambda z - \nu \int_0^t \frac{ds}{N(s,\sigma)} \tag{2.2}$$

reduces the partial differential equations (PDE) (1.2) *to the ODE*

$$AV'' + BV^2 - CV = K, \qquad V = U', \tag{2.3}$$

where

$$A = \sigma_1^3\beta \neq 0, \qquad B = \frac{(\kappa+\omega)\sigma_1^2\beta}{2} \neq 0, \qquad C = \nu\beta r + \mu\sigma_1\lambda, \tag{2.4}$$

and $K \in \mathbb{R}$ is an arbitrary constant of integration.

Proof. Since $D^{\sigma}_{N,t}\varsigma = N \cdot (-\nu/N) = -\nu$, the chain rule gives $\varphi_x = \sigma_1 U'$, $\varphi_{xx} = \sigma_1^2 U''$, $\varphi_{xxxy} = \sigma_1^3\beta U''''$, $\varphi_y = \beta U'$, $\varphi_{xy} = \sigma_1\beta U''$, $\varphi_{xz} = \sigma_1\lambda U''$, and $D^{\sigma}_{N,t}(\varphi_y) = -\nu\beta U''$. Substituting into (1.2) and grouping terms, we obtain

$$\sigma_1^3\beta U'''' + (\kappa+\omega)\sigma_1^2\beta U'U'' - (\nu\beta r + \mu\sigma_1\lambda)U'' = 0, \quad \text{i.e.,} \quad \frac{d}{d\varsigma}\Big(AU''' + B(U')^2 - CU'\Big) = 0.$$

Integrating once gives $AU''' + B(U')^2 - CU' = K$. We keep K arbitrary, because every value of K produces a solution of (1.2); with $V = U'$, this is (2.3). □

Remark 10. The kernel N enters only through the phase $\nu\tau(t)$. Therefore (2.3) and all of its solutions are independent of N, as predicted by Proposition 7.

Theorem 11. *Let $A, B \neq 0$ and let ϕ be a nonconstant solution of the auxiliary equation*

$$(\phi')^2 = h_0 + h_2\phi^2 + h_4\phi^4, \qquad h_4 \neq 0. \tag{2.5}$$

Then $V = s_0 + s_1\phi + s_2\phi^2$ solves (2.3) *if and only if*

$$s_1 = 0, \qquad s_2 = -\frac{6Ah_4}{B}, \qquad s_0 = \frac{C - 4Ah_2}{2B}, \qquad K = \frac{16A^2\left(h_2^2 - 3h_0h_4\right) - C^2}{4B}. \tag{2.6}$$

In particular, solutions with $K = 0$ exist if and only if the compatibility condition

$$C^2 = 16A^2\left(h_2^2 - 3h_0h_4\right) \tag{2.7}$$

holds. The corresponding solutions of (1.2) *are $\varphi = U(\varsigma)$, where $U' = V$ and ς is given by* (2.2).

Proof. Balancing the highest-order terms $V'' \sim \phi^{k+2}$ and $V^2 \sim \phi^{2k}$ gives $k = 2$. Differentiating (2.5) gives $\phi'' = h_2\phi + 2h_4\phi^3$. (This holds wherever $\phi' \neq 0$, and hence everywhere by continuity, because the zeros of ϕ' are isolated for nonconstant ϕ.) Substituting $V = s_0 + s_1\phi + s_2\phi^2$ into (2.3) and using (2.5) turns the left-hand side into a polynomial in ϕ. Equating its coefficients with those of K gives

$$\begin{aligned}
&\phi^4 : s_2(6Ah_4 + Bs_2) = 0, && \phi^3 : 2s_1(Ah_4 + Bs_2) = 0,\\
&\phi^2 : 4As_2h_2 + B(s_1^2 + 2s_0s_2) - Ca_2 = 0, && \phi^1 : s_1(Ah_2 + 2Bs_0 - C) = 0,\\
&\phi^0 : 2As_2h_0 + Bs_0^2 - Cs_0 = K.
\end{aligned}$$

For a nonconstant V, we need $s_2 \neq 0$, which gives $s_2 = -6Ah_4/B$. Then the ϕ^3 equation becomes $-10Ah_4s_1 = 0$, so $s_1 = 0$. The ϕ^2 equation then gives $s_0 = (C - 4Ah_2)/(2B)$, and the ϕ^1 equation is satisfied. Finally, substituting s_0 and s_2 into the ϕ^0 equation and simplifying gives the value of K in (2.6). Hence $K = 0$ is equivalent to (2.7). □

Remark 12. Theorem 11 separates the two possible situations. If (2.7) holds, the profiles solve the reduced equation with zero integration constant. If it does not hold, the same profiles are still exact solutions of the PDE (1.2), but of the reduction with the nonzero constant K given in (2.6). Throughout, we work with the squared auxiliary equation (2.5). For instance, $\phi = \operatorname{sech}\varsigma$ satisfies (2.5), but it does not satisfy the positive-root equation $\phi' = +\sqrt{\cdots}$ globally, because ϕ' changes sign at $\varsigma = 0$.

It is perfectly possible to reproduce all the cases obtained in [6] (which uses the conformable derivative) using the generalized local derivative D_N^σ. The key lies in the fact that the algebraic structure of the reduced ODE is identical; what changes is the definition of the wave variable ς (that is, the time scale). Recall that $N(t,\sigma)$ is the kernel of the generalized derivative; thus, if we choose $N(t,\sigma) = t^{1-\sigma}$, we recover the results of [6].

We now distinguish the dependent variables carefully: $V = U'$ is the derivative of the profile (it is not a wave speed), while $U = \varphi$ is the potential.

Theorem 13. *(Classification of generalized traveling wave solutions) Let $A, B \neq 0$ and let ς be given by* (2.2)*. For each family below, $V = U'$ solves* (2.3) *with the indicated value of K, and $\varphi = U(\varsigma)$ solves* (1.2) *for every admissible kernel N.*

(a) ***Bright/dark pulse and bounded kink*** *($h_0 = 0$, $h_2 = k^2 > 0$, $h_4 = -k^2$, $\phi = \operatorname{sech}(k\varsigma)$):*

$$V(\varsigma) = \frac{C - 4Ak^2}{2B} + \frac{6Ak^2}{B}\operatorname{sech}^2(k\varsigma), \qquad K = \frac{16A^2k^4 - C^2}{4B}, \tag{2.8}$$

$$U(\varsigma) = \frac{C - 4Ak^2}{2B}\varsigma + \frac{6Ak}{B}\tanh(k\varsigma) + U_0. \tag{2.9}$$

The derivative V is a localized pulse on the background $s_0 = (C - 4Ak^2)/(2B)$, of elevation type if $A/B > 0$ and of depression type if $A/B < 0$. The potential U is a bounded kink if and only if $s_0 = 0$, that is, $C = 4Ak^2$; in that case $K = 0$ and $U(\pm\infty) = U_0 \pm 6Ak/B$. If $s_0 \neq 0$, U contains the linear background $s_0\varsigma$ and is unbounded. The choice $h_0 = 1$, $h_2 = -2$, $h_4 = 1$, $\phi = \tanh\varsigma$, used in the original version, gives exactly the case $k = 1$ of (2.8)–(2.9)*, because* $\tanh^2 = 1 - \operatorname{sech}^2$.

(b) ***Cnoidal periodic waves*** *($h_0 = 1 - m^2$, $h_2 = 2m^2 - 1$, $h_4 = -m^2$, $\phi = \operatorname{cn}(\varsigma, m)$, $0 < m < 1$):*

$$V(\varsigma) = \frac{C - 4A(2m^2 - 1)}{2B} + \frac{6Am^2}{B}\operatorname{cn}^2(\varsigma, m), \qquad K = \frac{16A^2(m^4 - m^2 + 1) - C^2}{4B}.$$

These are bounded, nonsingular, and periodic, with period $4\mathbf{K}(m)$ in ϕ (and $2\mathbf{K}(m)$ in V). As $m \to 1^-$, they tend to the pulse (2.8) *with $k = 1$. As $m \to 0^+$ the amplitude $6Am^2/B$ tends to zero, so the trigonometric limit is the constant state $V = (C + 4A)/(2B)$ and not a nontrivial oscillatory wave.*

(c) ***Singular periodic waves*** *($h_0 = 0$, $h_2 = -k^2$, $h_4 = k^2$, $\phi = \sec(k\varsigma)$):*

$$V(\varsigma) = \frac{C + 4Ak^2}{2B} - \frac{6Ak^2}{B}\sec^2(k\varsigma), \qquad K = \frac{16A^2k^4 - C^2}{4B},$$

defined on each interval $|k\varsigma - n\pi| < \pi/2$, $n \in \mathbb{Z}$.

(d) ***Singular hyperbolic waves*** *($h_0 = 0$, $h_2 = k^2$, $h_4 = k^2$, $\phi = \operatorname{csch}(k\varsigma)$):*

$$V(\varsigma) = \frac{C - 4Ak^2}{2B} - \frac{6Ak^2}{B}\operatorname{csch}^2(k\varsigma), \qquad K = \frac{16A^2k^4 - C^2}{4B}, \qquad \varsigma \neq 0.$$

(e) ***Rational (singular) waves*** *($h_0 = h_2 = 0$, $h_4 = 1$, $\phi = -1/\varsigma$):*

$$V(\varsigma) = \frac{C}{2B} - \frac{6A}{B\varsigma^2}, \qquad K = -\frac{C^2}{4B}, \qquad \varsigma \neq 0.$$

This family satisfies the compatibility condition (2.7) *(i.e., $K = 0$) if and only if $C = 0$.*

Proof. In each case, a direct differentiation shows that ϕ satisfies (2.5) with the stated (h_0, h_2, h_4); for (b), we use $\mathrm{cn}' = -\mathrm{sn}\,\mathrm{dn}$, $\mathrm{sn}^2 = 1 - \mathrm{cn}^2$, and $\mathrm{dn}^2 = 1 - m^2 + m^2\mathrm{cn}^2$. The formulas then follow from (2.6). For (a), integrating $\mathrm{sech}^2(k\varsigma)$ gives (2.9), and the limits $\tanh(\pm\infty) = \pm 1$ give the boundedness criterion. We also checked every family numerically by evaluating the residual $AV'' + BV^2 - CV - K$ at sample points; the residuals are at round-off level ($\lesssim 10^{-10}$). □

Remark 14. The proof of all these cases is consistent because the generalized local derivative D_N^σ possesses the linearity property and the chain rule, which, for the traveling-wave change of variable, acts identically to the classical derivative, except for the time-scale factor $\frac{1}{N(t,\sigma)}$. Therefore, all the results in the work [6] are particular cases of this scheme, recoverable simply by assigning $N(t, \sigma) = t^{1-\sigma}$. The generalized version allows us to model media with nonstandard (nonuniform) time scales; as explained in Remark 8, it does not model memory.

3. Propagation under different kernels

By Proposition 7, the kernel only changes the clock. The following result makes the effect on the fronts precise.

Proposition 15 (Front kinematics)**.** *Fix y, z and a level ς_0 of the profile (for example, the crest of the pulse or the center of the kink). Its position along the x-axis is*

$$x_c(t) = \frac{\varsigma_0 - \beta y - \lambda z + \nu\,\tau(t)}{\sigma_1}, \qquad \dot{x}_c(t) = \frac{\nu}{\sigma_1 N(t,\sigma)}.$$

Let $0 < \sigma < 1$.

(i) $N = 1$: uniform motion, x_c is linear in t.

(ii) $N = t^{1-\sigma}$ (conformable, [6]): $\tau(t) = t^\sigma/\sigma$. The motion is sublinear; the speed is infinite at $t = 0^+$ and decays like $t^{\sigma-1}$.

(iii) $N = e^{(1-\sigma)t}$: $\tau(t) = (1 - e^{-(1-\sigma)t})/(1-\sigma)$. The front is arrested at the finite position $x_\infty = x_c(0) + \nu/(\sigma_1(1-\sigma))$, which it approaches exponentially: $x_\infty - x_c(t) = \nu e^{-(1-\sigma)t}/(\sigma_1(1-\sigma))$.

(iv) $N = E_\sigma(t^{-\sigma})$: The front starts from the rest ($\dot{x}_c(t) \sim \nu\sigma e^{-1/t}/\sigma_1$ as $t \to 0^+$), the speed increases monotonically to the classical value ν/σ_1, and the lag behind the classical front grows sublinearly:

$$t - \tau(t) \sim \frac{t^{1-\sigma}}{(1-\sigma)\Gamma(1+\sigma)}, \qquad t \to \infty.$$

Proof. The level set $\varsigma = \varsigma_0$ gives x_c, and $\tau' = 1/N$ gives $\dot{x}_c$. Cases (i)–(iii) follow by direct integration. For (iv), the properties of $\rho = 1/E_\sigma(t^{-\sigma})$ were listed after (1.1). Since $1 - \rho(t) = t^{-\sigma}/\Gamma(1+\sigma) + O(t^{-2\sigma})$ as $t \to \infty$ and $0 \le 1 - \rho \le 1$, integrating $1 - \rho$ over $[0, t]$ gives the stated asymptotics for $t - \tau(t) = \int_0^t (1 - \rho(s))\,ds$. □

Thus the kernel produces four qualitatively different regimes: uniform, sublinear, arrested, and delayed. Case (iii) is a precise mathematical form of the "wave trapping" mentioned in the original version: The entire classical evolution on $[0, 1/(1-\sigma))$ is compressed into the physical interval $[0, \infty)$. We stress that the profile is transported unchanged; there is no change of amplitude or width (Section 4).

Figure 1(a) illustrates the three-dimensional profile of the trial function at $t = 0.5$. Figure 1(b) compares the profiles corresponding to different fractional orders, showing the prescribed changes in amplitude. Figure 1(c) demonstrates the influence of the spatial variable z on the wave structure, while Figure 1(d) depicts its evolution over time. Figure 1(e) presents the nonlinear interaction between ϕ_{xy} and ϕ_x. Finally, Figure 1(f) shows an approximate representation of the Caputo fractional derivative term. These visualizations are illustrative and do not establish that the trial function satisfies the governing equation.

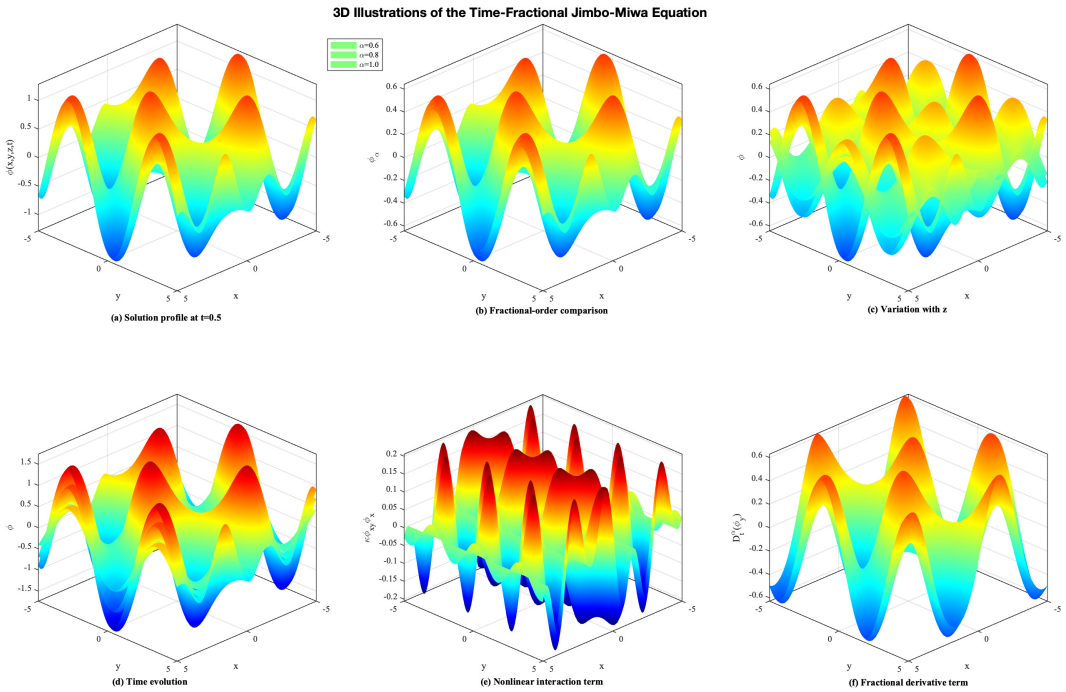


Figure 1. Three-dimensional visualization of the trial solution and its associated terms for the time-fractional JM equation.

Numerical settings for all figures. All figures are computed from the exact solutions; no PDE is solved numerically. We take $y = z = 0$, $\sigma_1 = \beta = \lambda = 1$, $\nu = r = 1$, $\kappa = \omega = \mu = 3$, so that $A = 1$, $B = 3$, $C = 4$. We take $k = 1$ in (2.8)-(2.9), so that $s_0 = 0$, $s_2 = 2$, $K = 0$, $V = 2\,\mathrm{sech}^2\,\varsigma$ and $U = 2\tanh\varsigma$ (a bounded kink). The kernel parameter is $\sigma = 0.7$ and the spatial window is $x \in [-8, 14]$ with 2001 points. For $N = 1$, $e^{(1-\sigma)t}$ and $t^{1-\sigma}$ the phase $\tau(t)$ is evaluated in closed form. For $N = E_\sigma(t^{-\sigma})$, E_σ is computed from the series (1.1) (log-sum-exp, 8000 terms) for $t^{-\sigma} \le 400$ and from the asymptotic formula otherwise, and $\tau(t)$ is obtained by adaptive Gauss-Kronrod quadrature (absolute tolerance 10^{-13}, relative tolerance 10^{-11}).

The six subplots illustrate different features of the trial function for the time-fractional JM equation. Figure 2(a) displays the solution profile, whereas Figure 2(b) compares its behavior for four fractional orders. Figure 2(c) presents the spatial profile at $z = 2$, and Figure 2(d) shows the wave profile at $t = 1$. Figure 2(e) depicts the nonlinear interaction term, while Figure 2(f) illustrates the fractional derivative contribution using an approximate Caputo derivative. These curves provide qualitative comparisons and do not establish exact solutions of the governing equation.

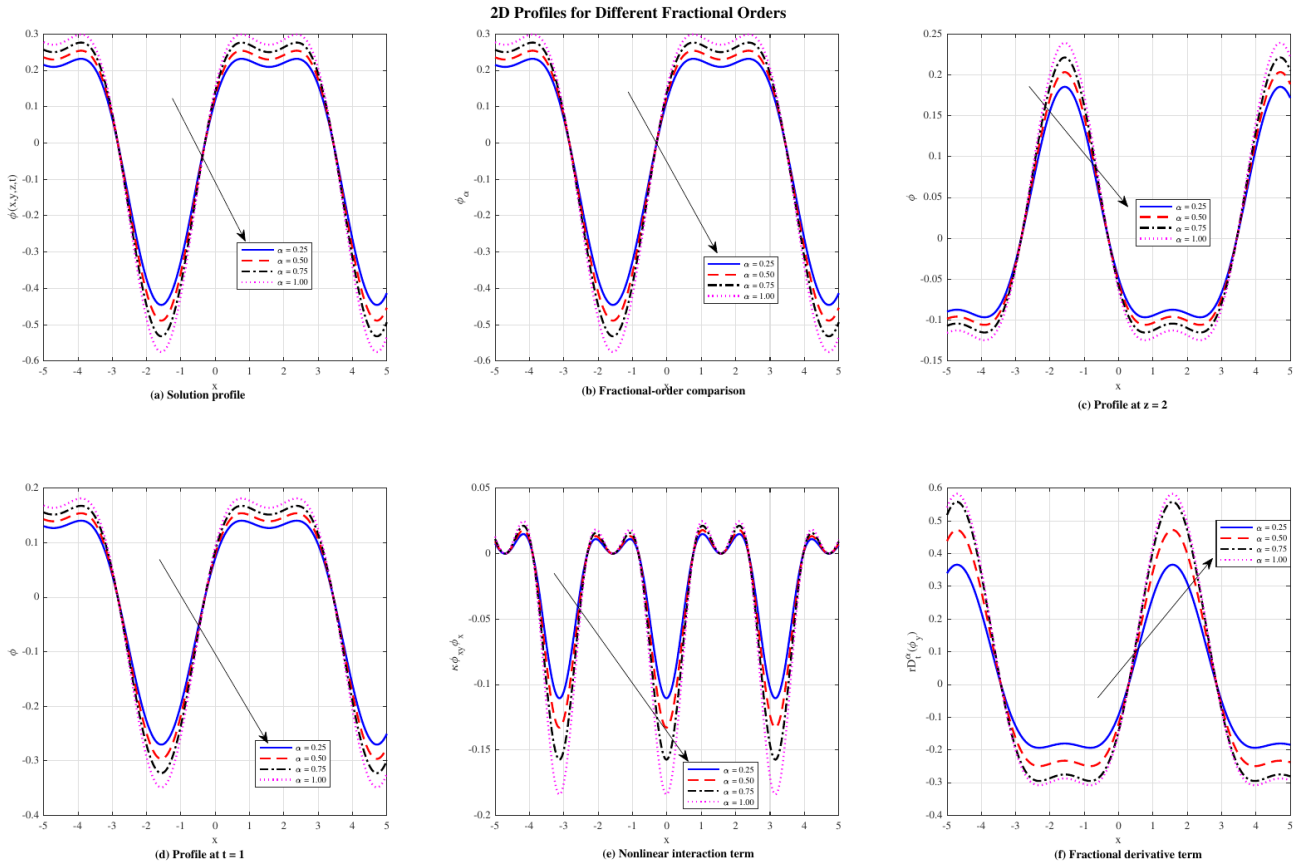


Figure 2. Three-dimensional visualization of the trial solution and its associated terms for the time-fractional JM equation.

Interpretation of Figures 2–5. For $N = 1$, the snapshots are equally spaced, and the kink and the pulse move at the constant speed v/σ_1. For $N = e^{(1-\sigma)t}$, the spacing between consecutive snapshots decreases exponentially, and the front accumulates at $x_\infty = 1/(1-\sigma) \approx 3.33$, in agreement with Proposition 15(iii). For $N = E_\sigma(t^{-\sigma})$, the front barely moves for small t (its speed is of order $e^{-1/t}$), then accelerates, and its speed approaches the classical value, while the accumulated lag behind the classical front keeps growing like $t^{1-\sigma}$. This is the opposite of the conformable weight, whose speed is largest at small times and decays. In all cases, the shape, amplitude, and width of the profiles are the same at all times, as expected from Proposition 7. The original version contained a three-panel contour plot and a three-dimensional surface plot; these were removed because they showed the same information less clearly than Figures 2–5. The original plotting code also replaced the Mittag-Leffler phase by the approximation t^σ/σ, which is the conformable phase. The figures above use the exact

Mittag-Leffler phase.

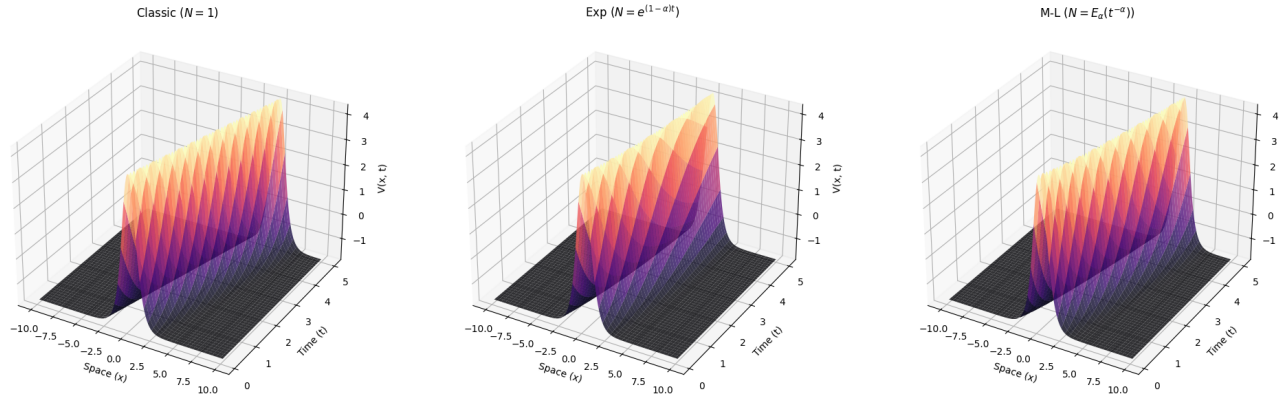


Figure 3. Bounded kink potential $\varphi(x, 0, 0, t) = U(\varsigma) = 2\tanh\varsigma$, $\varsigma = x - \nu\tau(t)$, at $t = 0, 2, 4, 6, 8$ for the three kernels. Parameters: $\sigma_1 = \beta = \lambda = \nu = r = 1$, $\kappa = \omega = \mu = 3$ ($A = 1$, $B = 3$, $C = 4$, $k = 1$, $K = 0$), $\sigma = 0.7$.

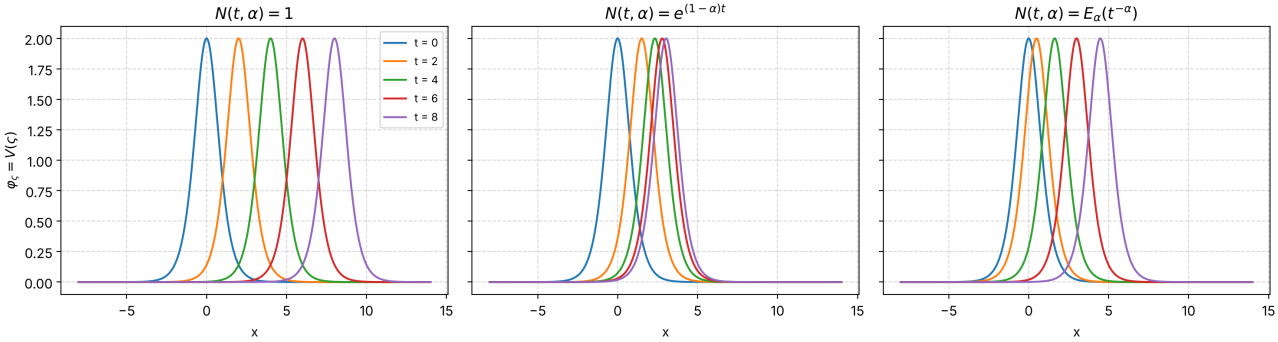


Figure 4. Bright pulse $V = \varphi_\varsigma = 2\,\mathrm{sech}^2\varsigma$, $\varsigma = x - \nu\tau(t)$, at $t = 0, 2, 4, 6, 8$ for the three kernels. Parameters as in Figure 3.

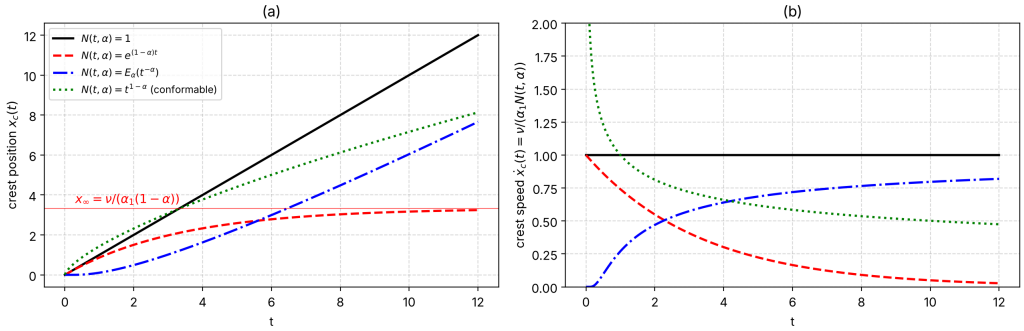


Figure 5. (a) Crest position $x_c(t) = \nu\tau(t)/\sigma_1$ and (b) crest speed $\dot{x}_c = \nu/(\sigma_1 N(t, \sigma))$ for $N = 1$, $e^{(1-\sigma)t}$, $E_\sigma(t^{-\sigma})$ and the conformable weight $t^{1-\sigma}$ of [6]; $\sigma = 0.7$, $\sigma_1 = \nu = 1$. The thin horizontal line in (a) is the arrest position $x_\infty = 1/(1-\sigma)$ of the exponential kernel.

4. Energy and entropy are kernel independent

The original version interpreted the slowing of the fronts as a loss of energy and an increase of entropy. A careful computation shows that this interpretation is not correct, and we have replaced that discussion with the following result.

Proposition 16. *Let $V(x,t) = a_0 + W(\sigma_1 x - \nu\tau(t))$ (with y, z fixed), where $W \in L^2(\mathbb{R})$, $W \not\equiv 0$. Define the background-subtracted energy and the Shannon entropy*

$$E(t) = \int_{\mathbb{R}} |V(x,t) - a_0|^2 \, dx, \qquad P(x,t) = \frac{|V(x,t) - a_0|^2}{E(t)}, \qquad S(t) = -\int_{\mathbb{R}} P \ln P \, dx.$$

Then $E(t) = |\sigma_1|^{-1}\|W\|_{L^2}^2$ and $S(t) = S(0)$ for all t and for every kernel N. For the pulse (2.8) *($W = a_2 \operatorname{sech}^2(k\,\cdot)$, $a_2 = 6Ak^2/B$), we have*

$$E = \frac{4a_2^2}{3k|\sigma_1|}, \qquad S = c_* - \ln(k|\sigma_1|), \qquad c_* = -\int_{\mathbb{R}} \tfrac{3}{4}\operatorname{sech}^4 u \, \ln(\tfrac{3}{4}\operatorname{sech}^4 u)\, du \approx 0.848427.$$

Proof. The change of variables $\xi = \sigma_1 x - \nu\tau(t)$ gives $dx = d\xi/|\sigma_1|$, so $E(t) = |\sigma_1|^{-1}\int W^2(\xi)\, d\xi$. Likewise, $P(x,t) = |\sigma_1|\, p(\xi)$ with $p = W^2/\|W\|^2$, so $S(t) = -\int p \ln p \, d\xi - \ln|\sigma_1|$; neither expression depends on t. The explicit values follow from $\int_{\mathbb{R}} \operatorname{sech}^4 u \, du = 4/3$ and the substitution $u = k\xi$. □

The background subtraction is necessary: If $a_0 \neq 0$, the integral of $|V|^2$ diverges. By Proposition 7, the same conclusion holds for any functional that is conserved by the classical JM flow: If $dQ/d\tau = 0$, then $dQ/dt = \rho\, dQ/d\tau = 0$. Hence, within the LGD model, no kernel produces energy dissipation or entropy production. What the kernel changes is the rate at which the conserved structure is transported, measured by the front speed $\dot{x}_c = \nu/(\sigma_1 N)$ shown in Figure 5(b). The quantity "$E(t) \propto v(t)^2$" used in the original version was simply the square of this speed, not an energy derived from the equation, and has been removed.

The four panels in Figure 6 illustrate candidate kink and anti-kink profiles for different fractional orders of the time-fractional JM equation. Figure 6(a) compares the kink waves, whereas Figure 6(b) presents the corresponding anti-kink profiles. Figure 6(c) displays the wave profiles at a selected time, and Figure 6(d) depicts the associated traveling-wave surfaces. The fractional order influences the wave position through the traveling coordinate. These profiles remain illustrative until their residuals are verified.

Remark 17. In the former Figure 6, the curves fluctuated with amplitude of order 10^{-10} around the exact value $S \approx 0.8484268$. This was a numerical artifact. The pulse was translated across a fixed truncated window $[-20, 20]$ (1000 points), and all grid points with $P \leq 10^{-10}$ were discarded before integration. As the pulse moves, the set of discarded points changes from one time step to the next, which causes jumps of the size of the threshold. Removing the threshold (or enlarging the domain) reduces the variation to $\sim 10^{-16}$. The value is the same for all kernels, including $N = 1$, in agreement with Proposition 16.

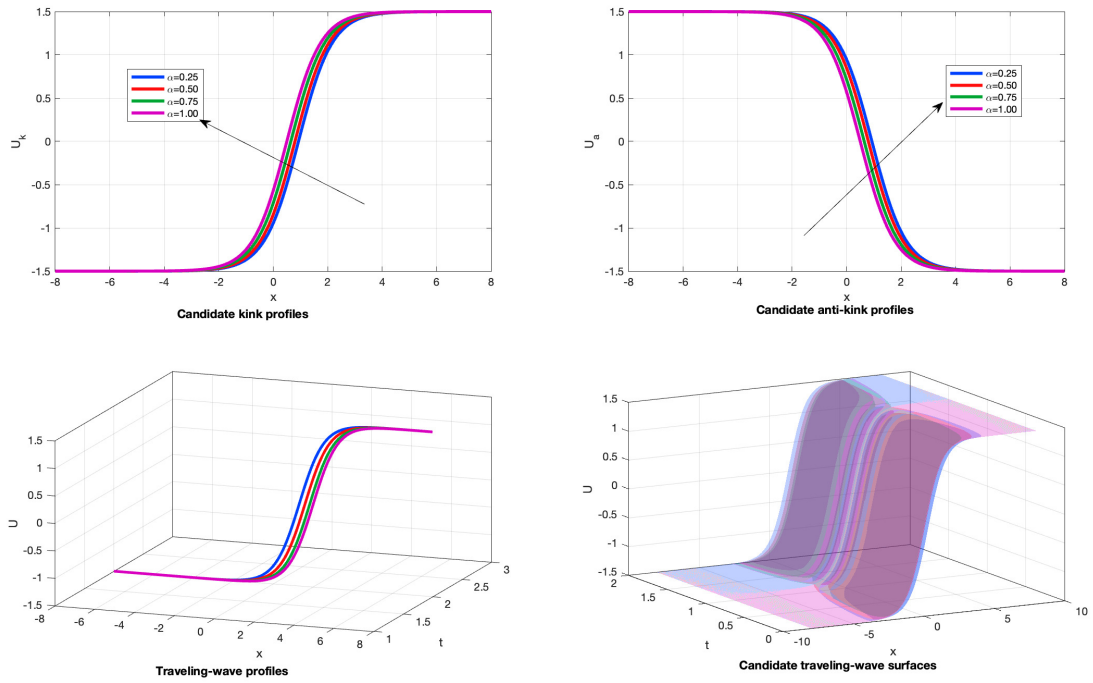


Figure 6. Candidate kink, anti-kink, and traveling-wave profiles for different fractional orders of the time-fractional JM equation.

5. Theoretical analysis

Lemma 18. *Under the assumptions of Definition 2,* $(\mathcal{D}_N^\beta(I), \|\cdot\|_{\mathcal{D}_N^\beta})$ *is a Banach space.*

Proof. Let $\{f_n\}$ be a Cauchy sequence on $\mathcal{D}_N^\beta(I)$. By the definition of the norm, $\{f_n\}$ and $\{D_N^\beta f_n\}$ are Cauchy sequences in $C(I)$ with the supremum norm. Since $C(I)$ is complete, there exist $f, g \in C(I)$ such that $f_n \to f$ and $D_N^\beta f_n \to g$ uniformly. Because $N \geq n_* > 0$, we have $f_n' = D_N^\beta f_n / N \to g/N$ uniformly on I. For every $t \in I$,

$$f_n(t) = f_n(0) + \int_0^t \frac{D_N^\beta f_n(s)}{N(s,\beta)} ds,$$

and the uniform convergence allows us to pass to the limit:

$$f(t) = f(0) + \int_0^t \frac{g(s)}{N(s,\beta)} ds.$$

Since g/N is continuous, the fundamental theorem of calculus gives $f \in C^1(I)$ with $f' = g/N$, that is, $f \in \mathcal{D}_N^\beta(I)$ and $D_N^\beta f = g$. Therefore $\|f_n - f\|_{\mathcal{D}_N^\beta} \to 0$. □

We now consider the Cauchy problem driven by the LGD

$$D_{N,t}^\sigma y(t) = F(t, y(t)), \quad t \in (0, T], \qquad y(0) = y_0 \in \mathbb{R}^n, \tag{5.1}$$

for a family of kernels $N(\cdot,\sigma)$, $\sigma \in J \subset (0,1]$. A solution is a function $y \in C(I;\mathbb{R}^n) \cap C^1((0,T];\mathbb{R}^n)$ satisfying (5.1) pointwise. We assume:

(H1) $\rho(t,\sigma) := 1/N(t,\sigma)$ extends to a continuous function on $I \times J$ with $0 \le \rho \le \rho^*$, and $\rho > 0$ on $(0,T] \times J$;

(H2) $F : I \times \mathbb{R}^n \to \mathbb{R}^n$ is continuous, and $|F(t,y) - F(t,z)| \le L_F|y-z|$; set $M_0 = \sup_{t\in I} |F(t,0)|$.

Assumption (H1) is satisfied by $N = 1$, by $N = e^{(1-\sigma)t}$ ($\rho^* = 1$), and by $N = E_\sigma(t^{-\sigma})$ ($\rho^* = 1$, $\rho(0,\sigma) = 0$), for any $T > 0$ and any compact $J \subset (0,1]$. The conformable weight $t^{1-\sigma}$ satisfies (H1) on $[t_0, T]$ with $t_0 > 0$.

Under (H1), y solves (5.1) if and only if $y \in C(I)$ is a fixed point of

$$\mathcal{T}_\sigma[y](t) = y_0 + \int_0^t \rho(s,\sigma)\, F(s,y(s))\, ds. \tag{5.2}$$

Indeed, if $y = \mathcal{T}_\sigma[y]$, then $y' = \rho F(t,y)$ is continuous on $(0,T]$, and multiplying by $N = 1/\rho$ gives (5.1). Conversely, a solution of (5.1) satisfies $y' = \rho F(t,y)$ on $(0,T]$, and integrating from 0, the integrand is bounded; and y is continuous at 0, which gives $y = \mathcal{T}_\sigma[y]$. Note that $D^\sigma_{N,t} y = F(\cdot, y)$ then extends continuously to I.

Theorem 19. *Under (H1) and (H2), problem* (5.1) *has a unique solution y_σ on I for each $\sigma \in J$, and*

$$\|y_\sigma\|_\infty \le R := (|y_0| + \rho^* M_0 T) e^{\rho^* L_F T}. \tag{5.3}$$

Proof. Let $\theta = 2\rho^* L_F$ (any $\theta > 0$ if $L_F = 0$) and equip $X = C(I;\mathbb{R}^n)$ with the Bielecki norm $\|y\|_\theta = \sup_{t\in I} e^{-\theta t}|y(t)|$. Since $e^{-\theta T}\|y\|_\infty \le \|y\|_\theta \le \|y\|_\infty$, this norm is equivalent to the supremum norm, so $(X, \|\cdot\|_\theta)$ is a Banach space. By (H1)–(H2), $\mathcal{T}_\sigma$ maps X into X. For $y, z \in X$ and $t \in I$,

$$|\mathcal{T}_\sigma[y](t) - \mathcal{T}_\sigma[z](t)| \le \rho^* L_F \int_0^t e^{\theta s}\, e^{-\theta s}|y(s) - z(s)|\, ds \le \rho^* L_F \|y - z\|_\theta \, \frac{e^{\theta t} - 1}{\theta}.$$

Multiplying by $e^{-\theta t}$ and taking the supremum gives $\|\mathcal{T}_\sigma[y] - \mathcal{T}_\sigma[z]\|_\theta \le \frac{\rho^* L_F}{\theta}\|y - z\|_\theta = \frac{1}{2}\|y - z\|_\theta$. By Banach's fixed point theorem, $\mathcal{T}_\sigma$ has a unique fixed point, which is the unique solution of (5.1). For the bound, $|y_\sigma(t)| \le |y_0| + \rho^* \int_0^t (M_0 + L_F|y_\sigma(s)|)\, ds$, and Grönwall's inequality gives (5.3). □

Theorem 20. *Assume (H1) and (H2) and let $M = M_0 + L_F R$, with R as in* (5.3). *For $\sigma_1', \sigma_2' \in J$ let $y_i = y_{\sigma_i'}$ and set*

$$\delta_\rho(\sigma_1', \sigma_2') = \int_0^T \left|\rho(s,\sigma_1') - \rho(s,\sigma_2')\right| ds.$$

Then

$$\|y_1 - y_2\|_\infty \le M\, e^{\rho^* L_F T}\, \delta_\rho(\sigma_1', \sigma_2'), \qquad \left\|D^{\sigma_1'}_{N,t} y_1 - D^{\sigma_2'}_{N,t} y_2\right\|_\infty \le L_F\, M\, e^{\rho^* L_F T}\, \delta_\rho(\sigma_1', \sigma_2'). \tag{5.4}$$

In particular, $\sigma \mapsto y_\sigma$ is continuous from J into $C(I)$. If, in addition,

(H3) $|\rho(t,\sigma_1') - \rho(t,\sigma_2')| \le L_\rho|\sigma_1' - \sigma_2'|$ for all $t \in I$, then $\|y_1 - y_2\|_\infty \le M\, T\, L_\rho\, e^{\rho^* L_F T}|\sigma_1' - \sigma_2'|$.

Proof. Let $e(t) = |y_1(t) - y_2(t)|$. By (5.2), we decompose the difference as

$$y_1(t) - y_2(t) = \underbrace{\int_0^t (\rho(s,\sigma_1') - \rho(s,\sigma_2'))F(s,y_1(s))\,ds}_{\text{kernel term}} + \underbrace{\int_0^t \rho(s,\sigma_2')(F(s,y_1(s)) - F(s,y_2(s)))ds}_{\text{dynamics term}}.$$

By (5.3), $|F(s,y_1(s))| \le M_0 + L_F|y_1(s)| \le M$, so the kernel term is bounded by $M\delta_\rho$. The dynamics term is bounded by $\rho^* L_F \int_0^t e(s)\,ds$. Thus $e(t) \le M\delta_\rho + \rho^* L_F \int_0^t e(s)\,ds$, and Grönwall's inequality gives the first estimate in (5.4). Since $D_{N,t}^{\sigma_i'} y_i = F(t,y_i)$, both LGD derivatives belong to the same space $C(I)$, and their difference is bounded by $L_F e(t)$; this gives the second estimate. Continuity in σ follows because $\delta_\rho \to 0$ as $\sigma_2' \to \sigma_1'$, by dominated convergence (ρ is continuous and bounded by ρ^*). Under (H3), $\delta_\rho \le T L_\rho |\sigma_1' - \sigma_2'|$. □

Example 21 (Verification of (H3))**.** For $N = e^{(1-\sigma)t}$ we have $\partial_\sigma \rho = t\,e^{-(1-\sigma)t} \in [0,T]$, so (H3) holds with $L_\rho = T$. For $N = E_\sigma(t^{-\sigma})$, the series (1.1) and its σ-derivative converge uniformly for (σ, z) in compact subsets of $(0,1]\times[0,\infty)$, so (H3) holds on $[t_0,T]$ for every $t_0 > 0$; on the whole interval $[0,T]$, the continuity statement of Theorem 20 (through δ_ρ) applies.

Corollary 22. *Let $U \in C^{j+1}(\mathbb{R})$ with bounded derivatives (for example, the bounded kink* (2.9) *with $C = 4Ak^2$). Let $\varphi_\sigma = U(\sigma_1 x + \beta y + \lambda z - \nu\tau_\sigma(t))$, where $\tau_\sigma(t) = \int_0^t \rho(s,\sigma)\,ds$. Then, for $0 \le i \le j$,*

$$\sup_{\mathbb{R}^3\times I} \left|\partial_x^i \varphi_{\sigma_1'} - \partial_x^i \varphi_{\sigma_2'}\right| \le |\sigma_1|^i \, \|U^{(i+1)}\|_\infty \, |\nu| \, \delta_\rho(\sigma_1', \sigma_2').$$

For the bounded kink with $i = 0$, the constant is $\|U'\|_\infty = 6Ak^2/B$.

Proof. The phase $\theta_\sigma = \nu\tau_\sigma$ solves (5.1) with $F \equiv \nu$, so $L_F = 0$ and $M = |\nu|$. Theorem 20 gives $|\theta_{\sigma_1'}(t) - \theta_{\sigma_2'}(t)| \le |\nu|\delta_\rho$, and the claim follows from the mean value theorem applied to $\partial_x^i U$. □

Remark 23. Theorem 20 and Corollary 22 establish *continuous (Lipschitz) dependence* of solutions on the kernel parameter. They do not prove structural stability in the sense of dynamical systems, nor orbital stability of solitons, and we do not claim either. We also note that the reduced equation (2.3) is an autonomous second-order ODE in ς that does not involve the LGD; written as the first-order system (V, V'), its local existence and uniqueness follow from the classical Picard theorem. Well-posedness of the full PDE (1.2) reduces, through Proposition 7, to that of the classical JM equation on the time interval $[0, \tau(T)]$.

All these results show that the solutions of the JM model under the LGD depend continuously on the kernel. A small change of σ produces a small change of the front position, with the explicit bound of Corollary 22.

6. Conclusions

The main results obtained can be summarized in the following points: The LGD is a local operator. For the JM equation, it is equivalent to the classical time derivative with respect to the reparametrized time $\tau(t) = \int_0^t ds/N(s,\sigma)$ (Proposition 7). It therefore describes media with a nonuniform time scale, not media with memory. The traveling-wave reduction keeps an integration constant K, and the

coefficients obey the compatibility relation (2.6). With explicit parameter restrictions, we obtained bright and dark pulses with their bounded kink potentials (bounded if and only if $C = 4Ak^2$), cnoidal waves (whose trigonometric limit is trivial), and singular periodic, hyperbolic, and rational waves. The conformable results of [6] are recovered with $N = t^{1-\sigma}$. The kernel leaves the profiles unchanged and controls only the motion of the fronts: The motion is uniform for $N = 1$, sublinear for the conformable weight, arrested at the finite position $x_\infty = x_c(0)+\nu/(\sigma_1(1-\sigma))$ for the exponential weight, and delayed with a power-law lag $\sim t^{1-\sigma}$ for the Mittag-Leffler weight. The energy and the Shannon entropy of the profiles are independent of time for every kernel, so the model produces no dissipation or entropy growth. Cauchy problems driven by the LGD have unique solutions, obtained by a contraction in a Bielecki-weighted Banach space, and these solutions depend Lipschitz-continuously on the kernel parameter, with explicit constants. Describing genuine memory or dissipation would require nonlocal operators or additional terms in the model; this is left for future work. Furthermore, this work sets a precedent for exploring other local differential operators (see, for example, [7, 21, 22]) in the analysis of other media.

Author contributions

Juan E. Nápoles V: Conceptualization, Methodology, Writing–original draft. Hadeel Bin Amer: Formal analysis, Validation. Aziz Khan: Visualization, Software, Writing–review and editing. Aiman Mukheimer: Supervision, Funding acquisition. Shahneela Pitafi: Investigation, Writing–review and editing. All authors have read and approved the final version of the manuscript for publication.

Use of Generative-AI tools declaration

The authors declare they have not used Artificial Intelligence (AI) tools in the creation of this article.

Acknowledgments

Aziz Khan and Aiman Mukheimer would like to thank Prince Sultan University for paying the APC and for the support through TAS research lab.

Conflict of interest

The authors declare no conflicts of interest.

References

1. I. Podlubny, *Fractional differential equations*, Vol. 198, New York: Academic Press, 1999. https://doi.org/10.1016/S0076-5392(99)X8001-5
2. R. Gorenflo, A. A. Kilbas, F. Mainardi, S. V. Rogosin, *Mittag-Leffler functions, related topics and applications*, 2 Eds., Springer Monographs in Mathematics, Berlin: Springer, 2020. https://doi.org/10.1007/978-3-662-61550-8

3. J. E. Nápoles Valdes, P. M. Guzmán, L. M. Lugo, A. Kashuri, The local generalized derivative and Mittag-Leffler function, *Sigma J. Eng. Nat. Sci.*, **38** (2020), 1007–1017.
4. A. Fleitas, J. E. Nápoles Valdes, J. M. Rodríguez, J. M. Sigarreta, Note on the generalized conformable derivative, *Rev. Unión Mat. Argent.*, **62** (2021), 443–457. https://doi.org/10.33044/revuma.1930
5. D. Zhao, M. Luo, General conformable fractional derivative and its physical interpretation, *Calcolo*, **54** (2017), 903–917. https://doi.org/10.1007/s10092-017-0213-8
6. M. Ahmad, P. A. Naik, M. Yavuz, A. Zada, Analyzing the soliton waves' behavior in the (3+1)-dimensional time-fractional Jimbo–Miwa equation, *Mod. Phys. Lett. B*, **40** (2026), 2650070. https://doi.org/10.1142/S0217984926500703
7. R. E. Castillo, J. E. Nápoles Valdes, H. Chaparro, Omega derivative, *Gulf J. Math.*, **16** (2024), 55–67. https://doi.org/10.56947/gjom.v16i1.1430
8. N. Yogeesh, S. I. Mohammad, J. Divyashree, N. Raja, A. Vasudevan, H. Long, Pesticide residue induced hepatotoxicity: determination for animal studies based on fuzzy logic, *Appl. Math. Inf. Sci.*, **19** (2025), 365–378. https://doi.org/10.18576/amis/190212
9. M. Farman, A. Talib, K. S. Nisar, A. Sambas, M. Bayram, M. Hafez, Investigation of ABPV predict dynamics infection in honeybee colony production: soft patterns multiscale modeling with fractional approach, *Ain Shams Eng. J.*, **16** (2025), 103626. https://doi.org/10.1016/j.asej.2025.103626
10. R. Khalil, M. Al Horani, A. Yousef, M. Sababheh, A new definition of fractional derivative, *J. Comput. Appl. Math.*, **264** (2014), 65–70. https://doi.org/10.1016/j.cam.2014.01.002
11. P. M. Guzmán, G. E. Langton, L. M. Lugo Motta Bittencourt, J. Medina, J. E. Nápoles Valdes, A new definition of a fractional derivative of local type, *J. Math. Anal.*, **9** (2018), 88–98.
12. F. Martínez, J. E. Nápoles Valdes, Towards a non-conformable fractional calculus of n-variables, *J. Math. Appl.*, **43** (2020), 87–98. https://doi.org/10.7862/rf.2020.6
13. H. Khan, H. B. Amer, W. F. Alfwzan, J. Alzabut, R. Thinakaran, Green energy generation dynamical system: fractal-fractional mathematical modeling with AI-driven data analysis, *Contemp. Math.*, **7** (2026), 3327–3349. https://doi.org/10.37256/cm.7320269372
14. H. Khan, H. B. Amer, R. Latif, W. F. Alfwzan, R. Thinakaran, Investigation of radioisotopes population dynamics by the help of modeling and artificial intelligence, *Fractals*, **34** (2026), 2640035. https://doi.org/10.1142/S0218348X26400359
15. H. Khan, H. B. Amer, W. F. Alfwzan, J. Alzabut, R. Thinakaran, AI-based data analysis of a fractal-fractional order contamination transportation and sedimentation model for rivers, *Fractals*, **34** (2026), 2640037. https://doi.org/10.1142/S0218348X26400372
16. L. M. Lugo, J. E. Nápoles Valdes, M. Vivas-Cortez, On the generalized Laplace's equation, *Appl. Math. Inf. Sci.*, **16** (2022), 169–176. https://doi.org/10.18576/amis/160204
17. M. Jimbo, T. Miwa, Solitons and infinite dimensional Lie algebras, *Publ. Res. Inst. Math. Sci.*, **19** (1983), 943–1001. https://doi.org/10.2977/prims/1195182017

18. T. Ling, H. Wang, Y. Wang, The (2+1)-dimensional time-fractional Kundu–Mukherjee–Naskar equation: Lie point symmetries, exact solutions and conservation laws, *Chinese J. Phys.*, **96** (2025), 700–715. https://doi.org/10.1016/j.cjph.2025.05.004

19. T. Ling, H. Wang, Y. H. Wang, The (2+1)-dimensional generalized fifth-order KdV equation in its time-fractional form: Lie point symmetries, exact solutions and conservation laws, *Mod. Phys. Lett. B*, **40** (2026), 2650007. https://doi.org/10.1142/S0217984926500077

20. H. Wang, T. Ling, Y. Wang, Symmetry analysis and fractional effects of the (2+1)-dimensional time-fractional Bogoyavlensky–Konoplechenko equation, *Phys. Lett. A*, **585** (2026), 131671. https://doi.org/10.1016/j.physleta.2026.131671

21. P. M. Guzmán, J. E. Nápoles Valdes, M. Vivas-Cortez, A new generalized derivative and related properties, *Appl. Math. Inf. Sci.*, **18** (2024), 923–932. https://doi.org/10.18576/amis/180501

22. M. Vivas-Cortez, L. M. Lugo, J. E. Nápoles Valdes, M. E. Samei, A multi-index generalized derivative: Some introductory notes, *Appl. Math. Inf. Sci.*, **16** (2022), 883–890. https://doi.org/10.18576/amis/160604



AIMS Press

© 2026 the Author(s), licensee AIMS Press. This is an open access article distributed under the terms of the Creative Commons Attribution License (http://creativecommons.org/licenses/by/4.0)